High-Fat Diet–Induced Adipocyte Cell Death Occurs Through a Cyclophilin D Intrinsic Signaling Pathway Independent of Adipose Tissue Inflammation

Daorong Feng,[1] Yan Tang,[1] Hyokjoon Kwon,[1] Haihong Zong,[1] Meredith Hawkins,[1] Richard N. Kitsis,[1,2,3] and Jeffrey E. Pessin[1,4]

OBJECTIVE—Previous studies have demonstrated that mice fed a high-fat diet (HFD) develop insulin resistance with proinflammatory macrophage infiltration into white adipose tissue. Concomitantly, adipocytes undergo programmed cell death with the loss of the adipocyte-specific lipid droplet protein perilipin, and the dead/dying adipocytes are surrounded by macrophages that are organized into crown-like structures. This study investigated whether adipocyte cell death provides the driving signal for macrophage inflammation or if inflammation induces adipocyte cell death.

RESEARCH DESIGN AND METHODS—Two knockout mouse models were used: granulocyte/monocyte-colony stimulating factor (GM-CSF)–null mice that are protected against HFD-induced adipose tissue inflammation and cyclophilin D (CyP-D)–null mice that are protected against adipocyte cell death. Mice were fed for 4–14 weeks with a 60% HFD, and different markers of cell death and inflammation were analyzed.

RESULTS—HFD induced a normal extent of adipocyte cell death in GM-CSF–null mice, despite a marked reduction in adipose tissue inflammation. Similarly, depletion of macrophages by clodronate treatment prevented HFD-induced adipose tissue inflammation without any affect on adipocyte cell death. However, CyP-D deficiency strongly protected adipocytes from HFD-induced cell death, without affecting adipose tissue inflammation.

CONCLUSIONS—These data demonstrate that HFD-induced adipocyte cell death is an intrinsic cellular response that is CyP-D dependent but is independent of macrophage infiltration/activation. *Diabetes* **60:2134–2143, 2011**

Multiple studies in mice have demonstrated that a high-fat diet (HFD) results in an adipose tissue inflammatory response that consists of dynamic changes in adipose tissue macrophages, neutrophils, mast cells, T cells, and more recently, eosinophils (1–7). For example, an HFD results in a small increase in anti-inflammatory macrophages (sometimes referred to as M2) but with a large increase in the amount of proinflammatory macrophages (sometimes referred to as M1), with secretion from macrophages and adipocytes of a variety of inhibitory insulin-signaling cytokines as well as additional macrophage-attracting chemokines. This inflammatory signaling cascade is thought to impair insulin signal transduction, predominantly through a blockade of insulin receptor substrate protein function that generates a state of insulin resistance (8). A critical physiologic role of this inflammatory response in insulin signaling was established because pharmacologic and genetic blockade of macrophage inflammation were both found to prevent HFD-induced insulin resistance but not the development of obesity (9).

In parallel with the development of insulin resistance and adipose tissue macrophage infiltration, macrophages have been observed to organize around dead and/or dying adipocytes, which been termed adipocyte crown-like (ACL) structures (10–12). The morphologic criteria show that the adipocytes within the ACL structures display characteristics of necrotic cell death (13–15). Other studies, however, have suggested that adipocytes undergo HFD-induced apoptotic cell death (16). In either case, macrophage infiltration and activation is generally assumed to result from the generation of cell death–mediated signals (13). However, in a variety of circumstances, the macrophages themselves generate death signals for target cells. For example, inflammatory macrophages promote myofibroblast proliferation and apoptosis in liver injury, and macrophage-related microglia can promote cell death in the retina through the production of nerve growth factor (17,18). Macrophages are also required for endothelial cell death during programmed regression of temporary capillary networks within the developing eye and induce programmed cell death through the paracrine release of Wnt7b to activate the vascular endothelial cell canonical Wnt pathway (19–21).

Thus, it remains an unresolved issue whether HFD induces adipocyte cell death that in turn generates an immune response resulting in macrophage infiltration/activation or whether macrophage infiltration per se can induce adipocyte cell death. To address this issue, we have taken advantage of two different genetic mouse models. Previous studies have demonstrated that macrophage-activation–deficient granulocyte/monocyte-colony stimulating factor (GM-CSF)–knockout mice prevent HFD-induced adipose tissue inflammation (22). On the other hand, cyclophilin D (CyP-D) is a mitochondrial matrix protein necessary for the formation of the mitochondrial membrane transition pore (MMTP) that is required for necrotic cell death, and cells of CyP-D–knockout mice are protected against this form of cell death (23,24).

RESEARCH DESIGN AND METHODS

Animals. Dr. Richard Stanley provided the GM-CSF–knockout ($GM\text{-}CSF^{-/-}$) mice with permission from Dr. Glenn Dranoff (25). CyP-D–null and C57BL/6 J mice were purchased from The Jackson Laboratory (Bar Harbor, ME). All mice were housed in a Barrier facility equipped with a 12-h light/dark cycle and maintained on a normal chow diet (NCD; 10% calories from fat) or an HFD (60% calories from fat) obtained from Research Diets Inc. (New Brunswick, NJ). The Albert Einstein College of Medicine Institutional Animal Care and Use Committee approved all animal studies.

Glucose tolerance tests and insulin tolerance tests. Mice underwent glucose (GTT) and insulin (ITT) tolerance tests after 4 and 8 weeks of NCD or HFD feeding. For the ITTs, mice were fasted for 4 h and injected with 1 unit of insulin/kg body weight. For GTTs, mice were fasted for 16 h and injected with 1 g/kg body weight of glucose. Blood was collected at various times, and glucose concentration was determined using a OneTouch glucose monitoring system (LifeScan, Inc., Milpitas, CA).

Clodronate ablation of macrophages. Liposome-encapsulated clodronate was obtained from Dr. Nico van Rooijen (Vrije Universiteit, the Netherlands). Mice (9 weeks old) were fed an HFD and concomitantly received 150 μL liposome-clodronate or an equivalent volume of liposomes containing PBS once per week for 8 weeks. Alternatively, to determine macrophage ablation on the reversibility of an HFD, mice were fed an HFD for 8 weeks and then injected with liposome-encapsulated clodronate or liposome PBS once per week for 7 weeks while being maintained on the HFD.

Cell culture. Murine 3T3-L1 preadipocyte culture and adipocyte differentiation were conducted as previously described (26). Fully differentiated 3T3-L1 adipocytes were placed over night in Dulbecco's modified Eagle's medium (DMEM) in the presence or absence of 10% serum and then incubated for 4 h with staurosporine, ionomycin, or H_2O_2 to induce adipocyte cell death.

Lentivirus short hairpin RNA knockdown in 3T3-L1 preadipocytes. MISSION lentivirus short hairpin RNA (shRNA) Bacterial Glycerol Stocks for CyP-D shRNA and empty vector control plasmids were obtained from Sigma-Aldrich (St. Louis, MO). The plasmid DNAs were purified using the HiSpeed Plasmid Maxi Kit (Qiagen, Valencia, CA) and were transfected into human embryonic kidney 293T cells along with Lentiviral Packaging Mix (Sigma-Aldrich) to produce lentivirus packed with shRNA per the manufacturer's instruction. 3T3-L1 preadipocytes (80% confluence) were infected with the lentivirus, selected by puromycin, and subjected to standard adipocyte differentiation.

Stromal vascular cell isolation and fluorescence-activated cell sorting analysis. Epididymal fat pads were dissected, minced in HEPES-buffered DMEM supplemented with 10 mg/mL fatty acid–free BSA. The tissue fragments were centrifuged at 1,000g for 10 min at 4°C to pellet erythrocytes and other blood cells, and the tissue suspension was incubated with Liberase TM (0.05 mg/mL, Roche, Indianapolis, IN) and 50 units/mL DNase I (Sigma-Aldrich) at 37°C in an orbital shaker (150 Hz) for 25 to 30 min. The digested samples were filtered through a sterile 250-μm nylon mesh, and the suspension was centrifuged at 1,000g for 5 min. The cell pellet containing the stromal vascular cell (SVC) was further incubated with RBC Lysis Buffer for 10 min before centrifugation (300g for 5 min) and resuspended in fluorescence-activated cell sorting (FACS) buffer (2% BSA in PBS). The SVCs were incubated with Fcγ receptor blocker for 10 min at 4°C before staining with fluorescently labeled primary antibodies for 20 min at 4°C. SVCs were analyzed using a FACSCanto II flow cytometer (BD Biosciences, San Jose, CA).

Total RNA extraction and quantitative RT-PCR. Adipose tissue total RNA was extracted using QIAzol Lysis Reagent, RNeasy Mini Kit and then digested with DNase I. First-strand cDNA was synthesized using Omniscript RT Kit with random primers and analyzed using the Mesa Green qPCR kit (Eurogentec) and Taqman system (Applied Biosystems, Foster City, CA).

Cathepsin D activity assay. Cathepsin D activity was determined by the SensoLyte 520 cathepsin D assay kit (AnaSpec, Fremont, CA). Frozen adipose tissue was ground in liquid nitrogen, and dithiothreitol-containing assay buffer was added. The supernatant from centrifuge (12,000g for 10 min at 4°C) was used for assay, according to the manufacturer's instructions, and normalized for total protein content.

Immunohistocytochemistry. Adipose tissue samples were fixed for 24 to 36 h at room temperature in zinc-formalin fixative and embedded in paraffin. Paraffin-embedded adipose tissue was sectioned, deparaffinized, and heated in antigen unmask solution for antigen retrieval, and then cooled, washed, and blocked with 10% goat serum in Tris-buffered saline with Tween (10 mmol/L Tris-HCl [pH 7.5], 150 mmol/L NaCl, 0.05% Tween-20). The sections were incubated overnight with F4/80 primary antibody and perilipin primary antibody. Fluorescence-conjugated secondary antibodies were applied for detection, and the sections were counterstained in ProLong Gold antifade reagent (Invitrogen, Carlsbad, CA) with DAPI.

Immunoblotting. Nuclear-associated high mobility group box 1 (HMGB1) protein in adipose tissue was determined by isolation of the epididymal adipose tissue by grinding the tissue into a powder in liquid nitrogen that was boiled directly in SDS buffer (10% SDS, 20% glycerol, and 125 mmol/L Tris-HCl [pH 6.8]) for 20 min. Total proteins were separated by 10% SDS-PAGE and transferred onto polyvinylidene fluoride membranes for immunoblotting.

To determine the amount of HMGB1 secretion in the 3T3-L1 cells, fully differentiated 3T3-L1 adipocyte cells (10–12 days) were incubated with each death inducer for 4 h. The proteins in 30 μL of the cell medium were separated by10% SDS-PAGE. Nuclear associated HMGB1 was determined by extraction of 3T3-L1 adipocytes using ProteoJET Mammalian Cell Lysis Reagent (Thermo Fisher Scientific, Waltham, MA).

Statistical analysis. The data were analyzed by one-way ANOVA, followed by post hoc analysis for comparisons between individual groups. Statistical analyses were made at a significance level of $P < 0.05$ using the SPSS 18.0 software (SPSS Inc, Chicago, IL). Identical letters in figures indicate datasets that are not statistically significant from each other.

RESULTS

GM-CSF–null mice are protected against HFD-induced insulin resistance and adipose tissue inflammation. Previous research has reported that GM-CSF–null mice are protected against HFD-induced insulin resistance concomitant with reduced adipose tissue inflammation (22). To establish that the GM-CSF–null mice display the same phenotypic characteristics under our experimental conditions, control wild-type and GM-CSF–null mice were fed an NCD or HFD for 4 weeks (Fig. 1). Intraperitoneal GTT demonstrated the expected impaired glucose tolerance in HFD-fed wild-type mice compared with wild-type mice maintained on an NCD (Fig. 1A). The NCD-fed GM-CSF–null mice displayed a small but statistically significant improved glucose tolerance compared with wild-type mice fed the NCD (Fig. 1A). Glucose tolerance in the HFD-fed GM-CSF–null mice was similar to NCD-fed wild-type mice, which was not statistically different, but more importantly, the GM-CSF–null mice were fully protected against HFD-induced glucose intolerance (Fig. 1A). The protection against HFD-induced glucose intolerance was a consequence of improved insulin sensitivity, because ITTs demonstrated reduced insulin sensitivity in wild-type mice fed the HFD but no significant differences between the wild-type mice fed the NCD and the GM-CSF–null mice fed NCD or HFD (Fig. 1B).

Thus, to determine if the protection against HFD-induced insulin resistance paralleled a reduction in adipose tissue inflammation, we next compared the relative adipose tissue content of proinflammatory macrophages. The percentage of F4/80+CD11c+ macrophages (Fig. 1C and E) and the absolute number of F4/80+CD11c+ macrophages (Fig. 1G) increased in adipose tissue after 4 weeks of the HFD. A further increase in the percentage and number of adipose tissue F4/80+CD11c+ macrophages was noted at 8 weeks (Fig. 1D, F, and H). In contrast, the GM-CSF–null mice fed the NCD displayed a substantial reduction in the amount of adipose tissue F4/80+CD11c+ macrophages at 4 (Fig. 1C, D, and G) and 8 weeks (Fig. 1E, F, and H) compared with the wild-type mice fed the NCD. Moreover, the induction of F4/80+CD11c+ macrophages was markedly reduced in GM-CSF–null mice after 4 (Fig. 1C, D, and G) or 8 weeks (Fig. 1E, F, and H) of the HFD. Although not examined in detail, GM-CSF mice fed the HFD for 14 weeks also demonstrated a marked reduction in F4/80+CD11c+ macrophages in adipose tissue compared with wild-type mice (Supplementary Fig. 1A). In addition, the wild-type and GM-CSF–null mice gained similar extents of body weight on the HFD (Supplementary Fig. 1B).

Consistent with the flow cytometry analysis, F4/80 and CD11c mRNA was increased in the mice fed an HFD for
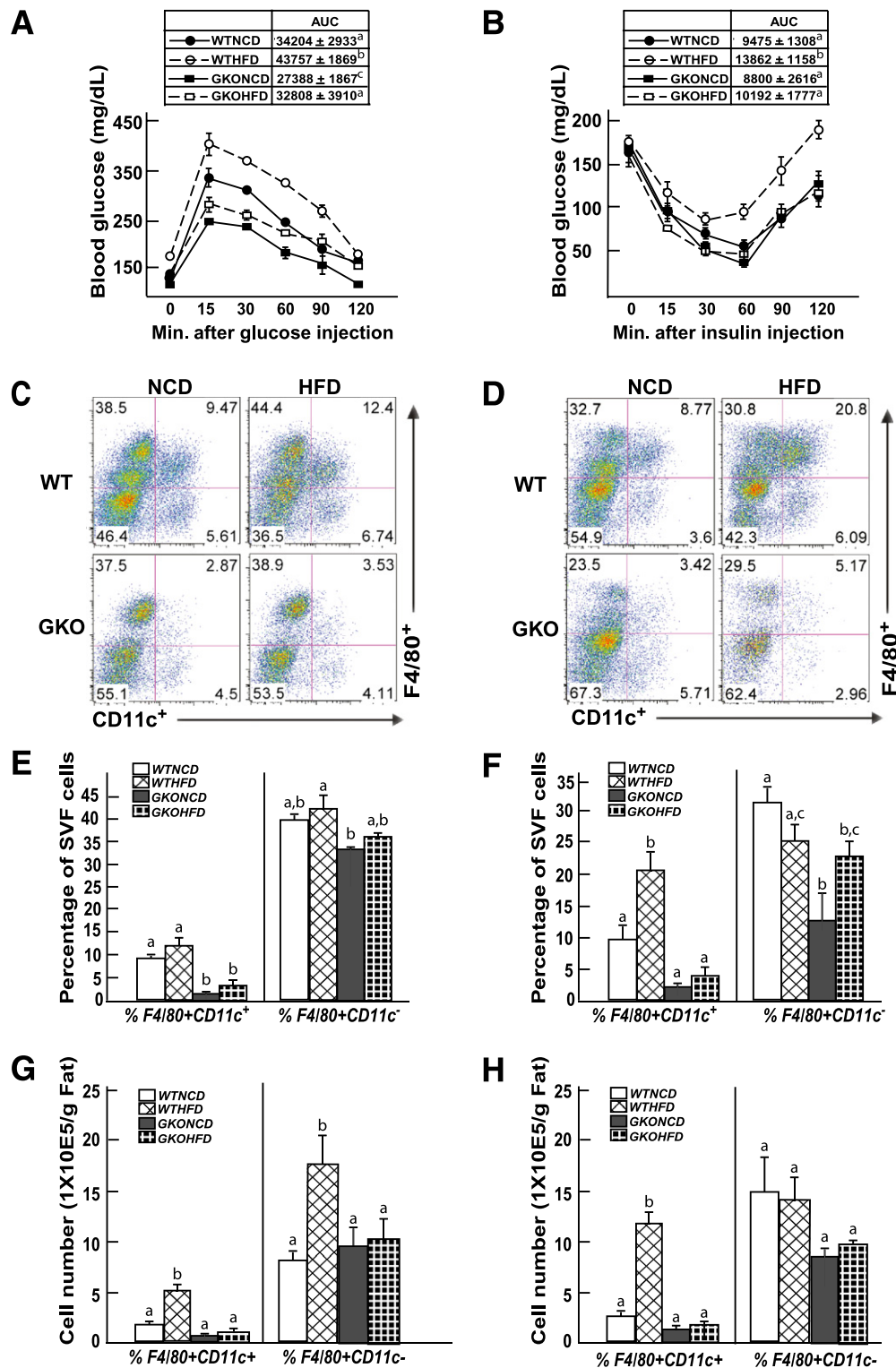
FIG. 1. GM-CSF–null mice are protected against HFD-induced glucose and insulin intolerance and against HFD-induced adipose tissue macrophage infiltration. Wild-type and GM-CSF–null 9-week-old male mice were fed NCD or HFD for 4 weeks, were fasted for 16 h (IPGTT) or 4 h (ITT), and blood was drawn for determination of fasting glucose and insulin levels. The mice were given an intraperitoneal injection of 1 g/kg glucose (*A*) or 1 unit/kg insulin (*B*), and blood glucose and insulin levels were determined at 15, 30, 60, 90, and 120 min. WTHFD, wild-type mice fed the HFD; WTNCD, wild-type mice fed the NCD; GKOHFD, GM-CSF–null mice fed the HFD; GKONCD, GM-CSF–null mice fed the NCD. Area under the curve (AUC) for each condition (*n* = 4 mice per group) is shown in the *insert*. Identical letters indicate values that are not statistically different from each other (*P* > 0.05). Wild-type and GM-CSF–null 9-week-old male mice were fed the NCD or HFD for 4 (*C, E, G*) or 8 (*D, F, H*) weeks. The stromal vascular fraction from an entire epididymal adipose tissue fat pad was isolated and subjected to flow cytometry analysis after labeling with F4/80 and CD11c antibodies, as described in RESEARCH DESIGN AND METHODS (*C, D*). The data obtained from three to five independent experiments were calculated for the percentage of F4/80+CD11c+ and F4/80+CD11c− (*E, F*) and the total number of F4/80+CD11c+ and F4/80+CD11c− cells (*G, H*). Data were analyzed as described in STATISTICAL ANALYSIS and are shown as the mean ± standard error of the mean. Identical letters indicate values that are not statistically different from each other (*P* > 0.05). (A high-quality digital representation of this figure is available in the online issue.)

4 (Supplementary Fig. 2A) and 8 (Supplementary Fig. 2B) weeks. Similarly, adipose tissue from the wild-type mice displayed increased expression of several cytokine/chemokines (monocyte chemoattractant protein-1, a disintegrin and metalloprotease domain 8, C-C chemokine receptor type 5, tumor necrosis factor-α, interleukin-6, and interferon-γ) at 4 and 8 weeks of the HFD. In contrast, these proinflammatory markers were significantly reduced in the GM-CSF–null mice, with little change after 4 or 8 weeks of the HFD. Together, these data demonstrate that the GM-CSF–null mice have a marked reduction of HFD-induced adipose tissue inflammation consistent with their protection against HFD-induced insulin resistance.

GM-CSF–null mice display a normal extent of HFD-induced adipocyte cell death. Having established that the GM-CSF–null mice provide a model system that prevents HFD-induced adipose tissue inflammation, we next

examined the relationship between adipose tissue inflammation and adipocyte cell death. Adipose tissue from NCD-fed wild-type mice had a baseline level of nuclei positive for transferase-mediated dUTP nick-end labeling (TUNEL), whereas TUNEL-positive nuclei were significantly increased after 14 weeks of the HFD (Fig. 2A and B). Similarly, NCD-fed GM-CSF–null mice also had a low level of TUNEL-positive nuclei. In contrast, the HFD in GM-CSF–null mice resulted in multiple TUNEL-positive adipose tissue nuclei that were similar in extent to the HFD-fed wild-type mice (Fig. 2A and B).

Because TUNEL staining cannot distinguish between adipocyte nuclei and nuclei from other cell types, we used immunofluorescence to detect the presence of the adipocyte-specific protein perilipin (Fig. 2C). NCD-fed wild-type and GM-CSF–null mice had a strong perilipin immunofluorescence signal. After 14 weeks of the HFD, wild-type adipose tissue had numerous regions of cells that
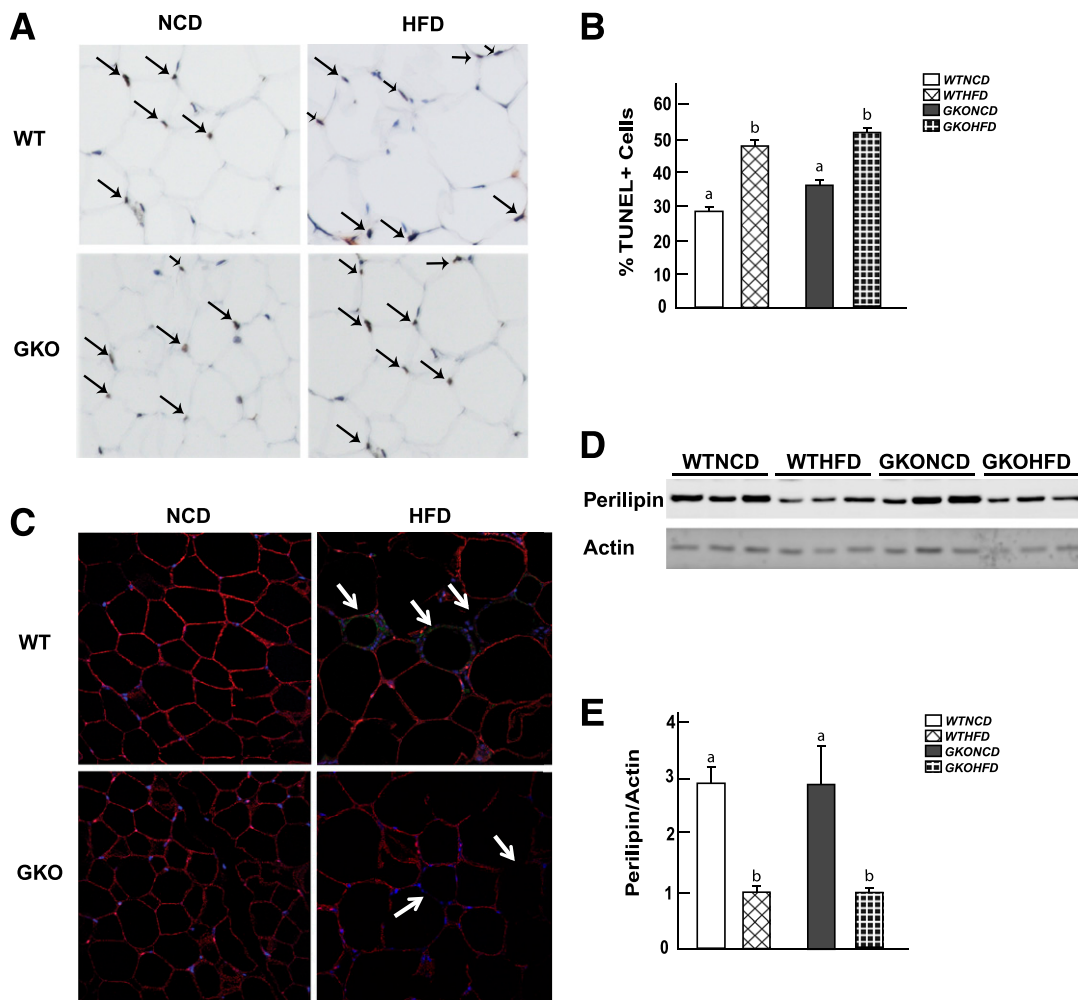

FIG. 2. TUNEL-positive cells increased in fixed epididymal tissue after 14 weeks of an HFD in wild-type and GM-CSF–null adipose tissue. Adipose tissue from wild-type and GM-CSF–null mice fed an NCD or HFD for 14 weeks was fixed and subjected to TUNEL staining. A: Dark brown nuclei are TUNEL-positive cells, and light blue is normal nuclei staining. B: Quantitated TUNEL-positive cells. Data shown are the mean ± standard error of the mean for three to six mice per group, with 200–500 nuclei per counted per individual mouse section. Identical letters indicate values that are not statistically different from each other (P > 0.05). C: Adipose tissue was subjected to immunofluorescence microscopy for perilipin expression using a secondary red antibody, F4/80 expression using a secondary green antibody, and nuclei by DAPI staining (blue). The white arrows indicate the cells with loss of perilipin expression. D: Adipose tissue (from three independent mice per condition) was extracted and immunoblotted for perilipin and actin. E: Laser scanning densitometry of the immunoblots was used to quantify the ratio of perilipin expression normalized for actin. Data shown are the mean ± standard error of the mean for four to six mice per group. Identical letters indicate values that are not statistically different from each other (P > 0.05). WTHFD, wild-type mice fed the HFD; WTNCD, wild-type mice fed the NCD; GKOHFD, GM-CSF–null mice fed the HFD; GKONCD, GM-CSF–null mice fed the NCD. (A high-quality digital representation of this figure is available in the online issue.)

were devoid of perilipin labeling, and these regions were typically surrounded by multinuclei (DAPI staining) indicative of ACL structures. Although a similar extent of perilipin-negative adipocytes were observed in the HFD-fed GM-CSF–null mice, there was no apparent ACL structure, consistent with the GM-CSF–null mice unable to display a macrophage inflammatory response.

Because TUNEL staining and perilipin immunofluorescence are not quantitative measures of adipocyte cell death and are highly dependent on the tissue section examined, we extracted whole adipose tissue fat pads and quantified the relative protein amounts of perilipin by immunoblotting (Fig. 2D and E). In this case, a relatively high percentage of the adipocyte population needs to undergo cell death to detect a decrease in protein levels. As such, we did not observe any significant decrease in perilipin

protein levels after 4 or 8 weeks of the HFD (data not shown) and, therefore, extended the time of the HFD to 14 weeks to increase the amount of adipocyte cell death. Under these conditions, the HFD induced a reduction in total adipose tissue perilipin protein levels in wild-type and GM-CSF–null mice compared with respective mice fed the NCD.

To further examine adipocyte cell death at earlier times after the HFD, we next assayed for cathepsin D activity, which is released from lysosomes (27). Cathepsin D activity was increased to the same extent in adipose tissue extracts after 4 weeks in the HFD-fed mice compared with NCD-fed wild-type and GM-CSF–null mice (Fig. 3A). The amount of cathepsin D activity was further increased after 8 weeks of the HFD and again was similar between wild-type and GM-CSF–null mice (Fig. 3B).
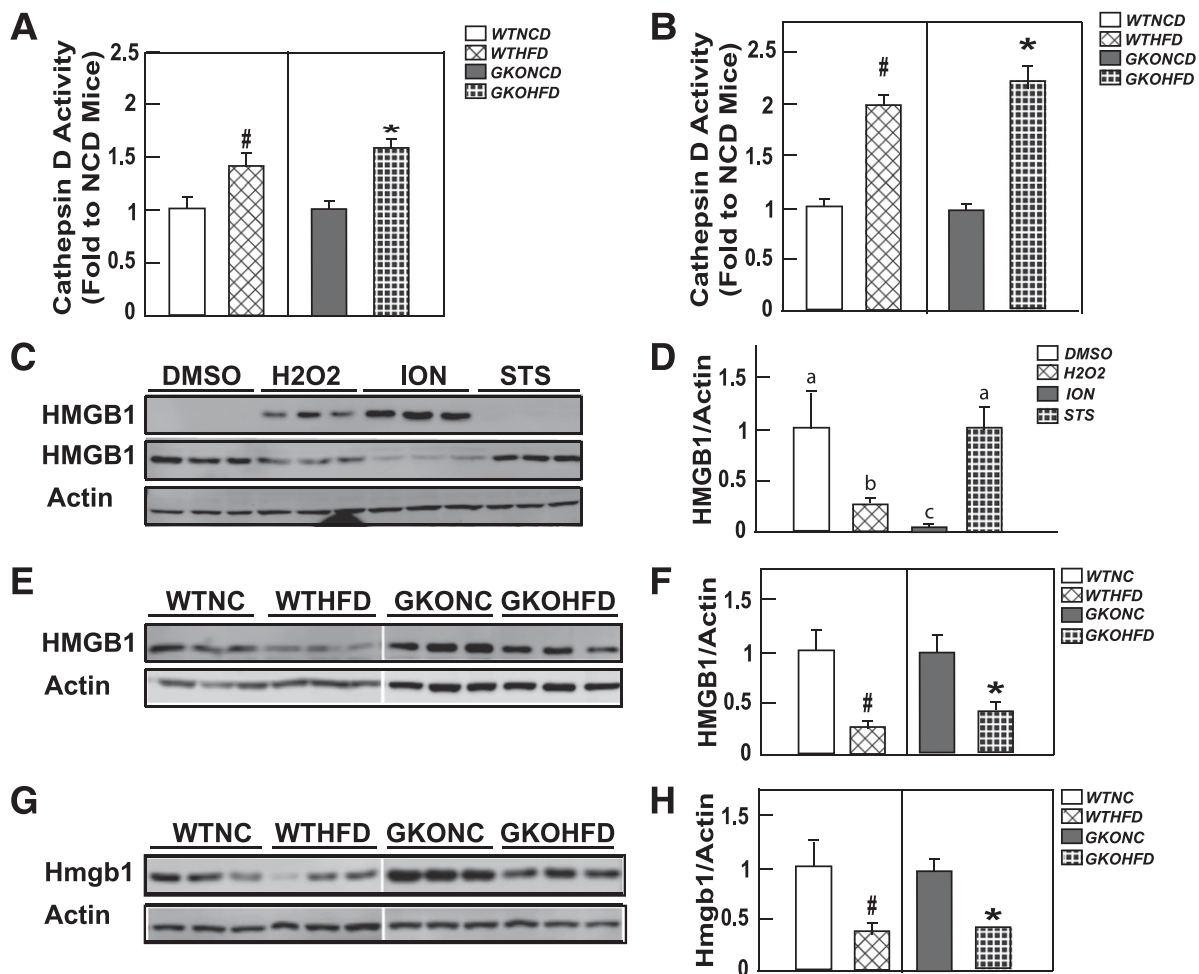

FIG. 3. Wild-type and GM-CSF mice fed the HFD display a similar increase in adipose tissue extract cathepsin D activity and HMGB1 release. Wild-type and GM-CSF–null male mice at 9 weeks of age were fed NCD or HFD for 4 (A) or 8 (B) weeks. Adipose tissue extracts from an entire epididymal adipose tissue fat pad were prepared and assayed for cathepsin D activity, as described in RESEARCH DESIGN AND METHODS. Cathepsin D activity of the HFD adipose tissue extracts was normalized to their respective NCD adipose tissue extracts. Data shown are the mean ± standard error of the mean for three to seven mice per group. C and D: 3T3-L1 cells were differentiated for 12 days to generate fully differentiated adipocytes as described in RESEARCH DESIGN AND METHODS. The cells were then treated for 1 h with vehicle (DMSO), 500 μmol/L H₂O₂, 2 μmol/L ION, or 1 μmol/L STS in serum-free DMEM medium. Then, 30 μL of the culture medium was immunoblotted for HMGB1 (upper panel). The cultured adipocytes were extracted, and 20 μg of protein was immunoblotted for HMBG1 and β-actin as a loading control. This is a representative immunoblot performed in triplicate. E–H: Wild-type and GM-CSF–null male 9-week-old mice were fed the NCD or HFD for 4 (E, F) or 8 (G and H) weeks. Adipose tissue extracts from an entire epididymal adipose tissue fat pad were prepared and immunoblotted for the presence of HMGB1 and actin as a loading control. These are representative immunoblots from three independent animals for each group. The right panels show densitometric quantification of the relative HMBG1/actin levels. For comparison, the ratios from the NCD mice were normalized to 1.0. Data shown are the mean ± standard error of the mean for three to five mice per group. In panels B, F, and H, the # and * symbols indicate statistical significance (P < 0.05) by Student t test. Data shown in panel D were analyzed as described in STATISTICAL ANALYSIS. Identical letters indicate values that are not statistically different from each other (P > 0.05).

Another assay for cell death is the nuclear release and accumulation of the HMGB1 protein in extracellular fluid (28). Typically, the release of HMGB1 is quantified in the medium of cells in culture. However, we have been unable to detect HMGB1 in the plasma or interstitial fluid around the adipose tissue in vivo (data not shown). Therefore, we first validated an analysis of nuclear HMGB1 levels in fully differentiated 3T3-L1 adipocytes. Untreated cultured 3T3-L1 adipocytes displayed essentially undetectable levels of HMGB1 in the medium, whereas nuclear HMGB1 was readily measured by immunoblotting (Fig. 3C). Treatment of 3T3-L1 adipocytes with the necrotic inducers H_2O_2 or the calcium ionophore ionomycin (ION) resulted in a substantial accumulation of HMGB1 in the medium, with a concomitant decrease in the nuclear fraction. In contrast, the apoptotic cell death–inducer staurosporine (STS) had no effect on the medium release of HMGB1, and the nuclear level was identical to that of untreated cells (Fig. 3D).

We next determined the nuclear levels of HMGB1 in adipose tissue (Fig. 3E–H). A two- to threefold decrease was noted in adipose tissue nuclear HMGB1 levels in wild-type mice fed an HFD for 4 (Fig. 3E and F) or 8 (Fig. 3G and H) weeks compared with the NCD-fed mice. A similar extent of nuclear HMGB1 levels also occurred in the adipose tissue from GM-CSF–null mice fed an HFD for 4 and 8 weeks, indicating that HFD enhanced adipocyte cell death in wild-type and GM-CSF–null mice.

Because GM-CSF–null mice displayed reduced HFD-induced macrophage infiltration into adipose tissue without any significant change in adipocyte cell death, we checked an alternative model to block adipose tissue inflammation. Mice treated with liposome-clodronate and concomitantly fed an HFD for 8 weeks displayed a marked reduction in the extent of adipose tissue inflammation (Fig. 4A). Despite the reduction in adipose tissue inflammation, the adipocytes still underwent an HFD-induced cell death, as detected by the loss of perilipin and adipose triglyceride lipase (ATGL) protein levels (Fig. 4C), and by TUNEL staining (Fig. 4E and G). In parallel, a marked reversal of adipose tissue inflammation also occurred in mice fed an HFD for 8 weeks, and then treated with liposome-clodronate for an additional 7 weeks while concomitantly maintained on the HFD (Fig. 4B), with a similar extent of adipocyte cell death by perilipin and ATGL protein levels (Fig. 4D) and TUNEL staining (Fig. 4F and H).

3T3-L1 adipocytes are resistant to apoptotic but are sensitive to necrotic cell death inducers. Figure 3 shows that STS was a poor inducer of 3T3-L1 adipocyte HMGB1 release, suggesting that adipocytes are resistant to STS-stimulated programmed cell death. Because STS is a well-established apoptotic inducer in cultured fibroblasts, we examined the STS sensitivity during 3T3-L1 adipocyte differentiation by using caspase 3 proteolytic cleavage as a marker for the induction of apoptosis (Fig. 5A). Treatment
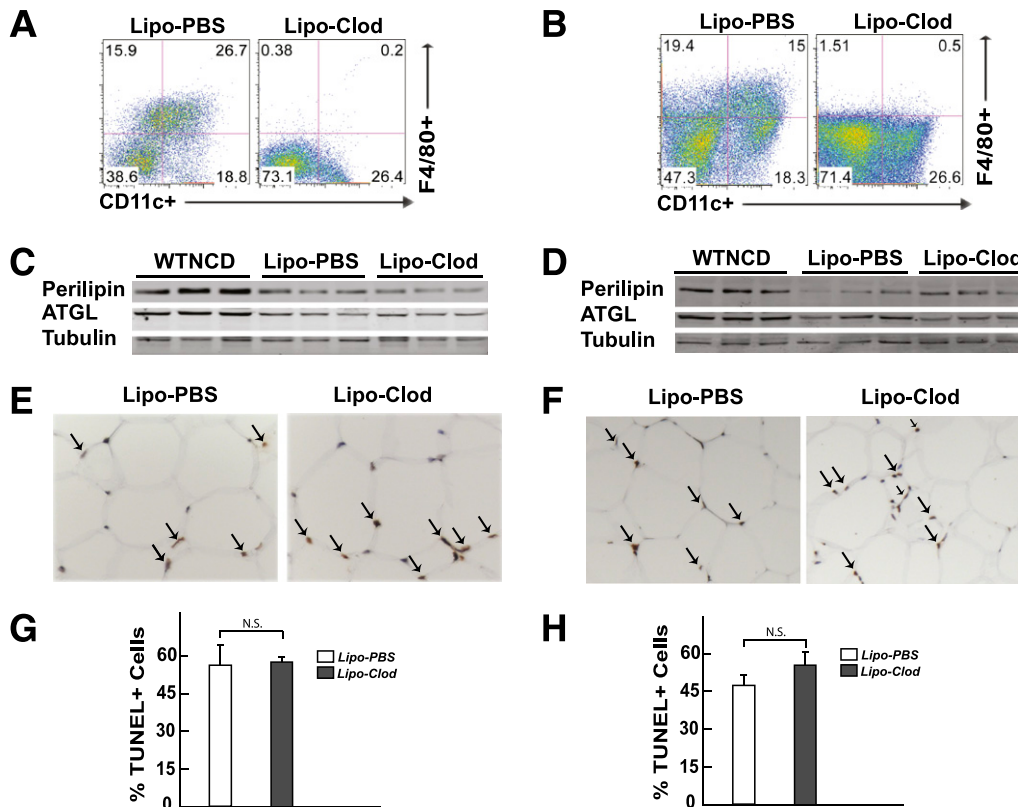

FIG. 4. Macrophage depletion by liposome clodronate had no effect on HFD-induced adipocyte cell death. Wild-type mice fed an NCD (WTNCD) were then fed an HFD and concomitantly injected weekly with liposome PBS or liposome clodronate for 8 weeks (*A, C, E, G*). Mice fed an HFD for 8 weeks were injected weekly with liposome PBS or liposome clodronate for an additional 7 weeks (*B, D, F, H*). These mice were continually maintained on the HFD. *A* and *B*: Representative FACS analyses of the stromal vascular fraction (SVF) isolated from epididymal adipose tissue from a total of four to seven independent determinations. *C* and *D*: Adipose tissue from three independent mice was extracted and immunoblotted for perilipin, ATGL, and actin. *E* and *F*: A representative TUNEL staining section shows positive nuclei (arrows). *G* and *H*: Quantification of TUNEL-positive cells are mean ± standard error of the mean for four to seven mice per group with 200–500 nuclei per counted per individual mouse section. N.S. as determined by Student *t* test. (A high-quality digital representation of this figure is available in the online issue.)
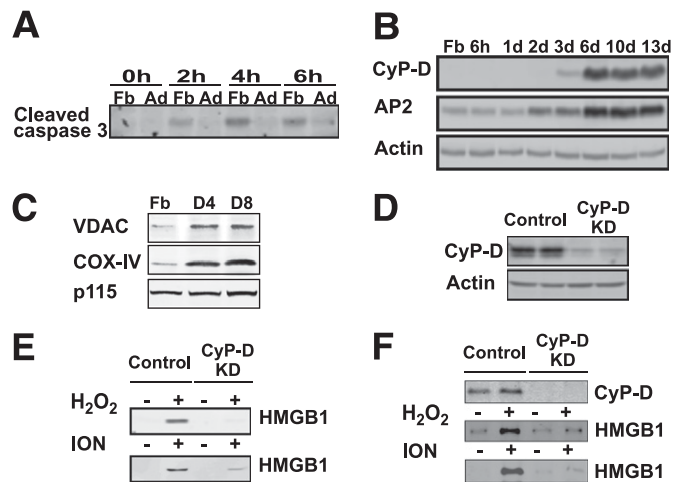
FIG. 5. Differentiated 3T3-L1 adipocytes are sensitive to CyP-D–dependent necrotic cell death. *A*: 3T3-L1 fibroblasts (Fb) and differentiated 3T3-L1 adipocytes (Ad) were treated with 1 μmol/L STS for the time indicated. The formation of proteolytic processed caspase 3 was detected by immunoblotting with a cleaved caspase 3–specific antibody. *B*: Cell extracts were prepared from 3T3-L1 fibroblasts and at different times after induction of 3T3-L1 adipogenesis. The induction of CyP-D protein was determined by immunoblotting and compared with the induction of the aP2 protein and actin as a loading control. *C*: Cell extracts were prepared from 3T3-L1 Fbs and after 4 (D4) and 8 (D8) days of adipocyte differentiation. The extracts were immunoblotted for the VDAC, COX-IV, and the p115 protein as a loading control. *D*: Cell extracts were prepared from differentiated 3T3-L1 adipocytes that were infected with a control lentivirus (MISSION control vector, two representative cell lines) and from cells infected with shRNA directed against CyP-D (clones of 638 and 710, two representative cell lines). Total cell extracts were immunoblotted for CyP-D and β-actin as a loading control. *E*: Control and CyP-D–knockdown (KD) cells were differentiated for 8 days and incubated for 24 h in the absence of serum. The cells were then treated with and without H_2O_2 (30 mmol/L) or ION (2 μmol/L) for 4 h. Cell extracts were prepared and immunoblotted for the presence of HMGB1 released into the cell medium. *F*: Control and CyP-D–knockdown cells were differentiated for 8 days and incubated with and without H_2O_2 (30 mmol/L) or ION (2 μmol/L) for 4 h in the presence of 10% FCS. Cell extracts were prepared and immunoblotted for CyP-D and for the presence of HMGB1 released into the cell medium.

of 3T3-L1 fibroblasts with STS for 2, 4, or 6 h resulted in the production of cleaved (activated) caspase 3. In contrast, differentiated adipocytes were highly resistant to STS-stimulated caspase 3 cleavage.

Previous studies in cardiac muscle have reported that the mitochondrial matrix protein cyclophilin D (CyP-D) is required for programmed necrotic cell death (29–31). Because 3T3-L1 fibroblasts are sensitive to an apoptotic inducer (STS) but not 3T3-L1 adipocytes, whereas 3T3-L1 adipocytes were sensitive to necrotic cell death inducers (H_2O_2 and ION), we determined the expression of the CyP-D protein during adipogenesis. Figure 5*B* demonstrates that the CyP-D protein is markedly induced during 3T3-L1 adipocyte differentiation. The increase in CyP-D protein levels during adipogenesis also correlated with increased expression of the mitochondrial markers voltage-dependent anion-selective channel (VADC) and cytochrome c oxidase subunit IV (COX-IV), suggesting that the induction of these proteins actually reflects an increase in mitochondrial mass that occurs during adipocyte differentiation (Fig. 5*C*).

Stable CyP-D–knockdown cell lines were generated using lentivirus shRNA (Fig. 5*D*), and these cells were protected against both H_2O_2- and ION-induced release of HMGB1 (Fig. 5*E*). Importantly, the CyP-D–knockdown cells were able to differentiate normally into an adipocyte phenotype, as demonstrated by the equal accumulation of

neutral lipid droplets (Supplementary Fig. 3). Moreover, the protection against H_2O_2- and ION-mediated adipocyte HMGB1 release by the loss of CyP-D occurred in the absence (Fig. 5*E*) and in the presence of serum (Fig. 5*F*).

CyP-D–null mice are protected against HFD-induced adipocyte cell death but display typical insulin resistance and adipose tissue inflammation. Because cultured adipocytes are resistant to apoptosis-induced cell death but are apparently sensitive to necrotic cell death inducers, concomitant with the induction of CyP-D, we hypothesized that HFD-induced adipocyte cell death in vivo may depend on CyP-D. We examined this possibility by first characterizing the glucose and insulin tolerance of CyP-D–null mice fed an HFD (Fig. 6). In contrast to GM-CSF–null mice, the CyP-D–null mice developed glucose and insulin intolerance when fed an HFD to a similar extent as wild-type mice (Fig. 6*A* and *B*). The insulin intolerance of HFD-fed wild-type and CyP-D–null mice is consistent with the development of peripheral tissue insulin resistance. As expected, HFD-fed wild-type mice displayed adipocyte cell death as assessed by decreased levels of the adipocyte-specific proteins perilipin, ATGL, and phosphodiesterase 3B (PDE3B; Fig. 6*C*). However, the expression levels of perilipin, ATGL, and PDE3B proteins did not change in the HFD-fed CYP-D–null mice, indicating protection against HFD-induced cell death despite an equal gain in body weight (Fig. 6*D*).

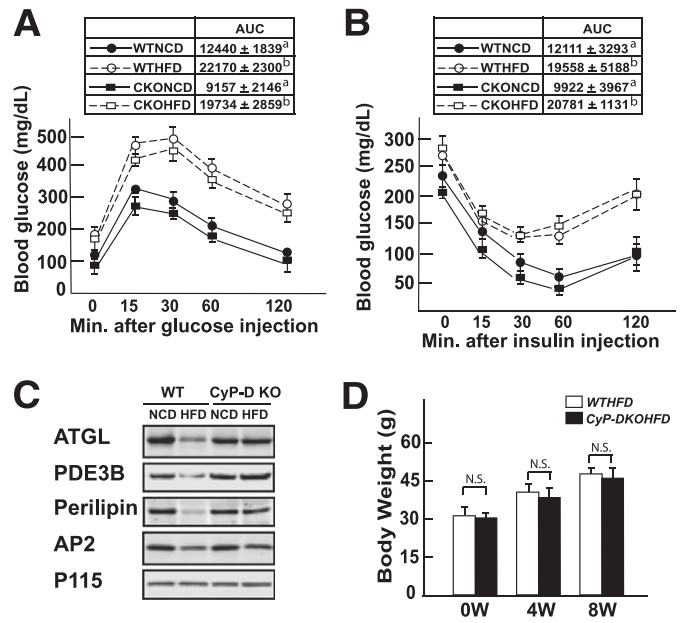FIG. 6. CyP-D mice are protected against HFD-induced adipocyte cell death but display glucose intolerance and insulin resistance. Wild-type and CyP-D–null 9-week-old male mice were fed an NCD or HFD for 9 weeks and then fasted for 16 h (IPGTT) or 5 h (ITT), and blood was drawn for determination of fasting glucose and insulin levels. The mice were given an intraperitoneal injection of 1 g/kg glucose (*A*) or 1 unit/kg insulin (*B*), and blood glucose and insulin levels were determined at 15, 30, 60 and 120 min. WTNCD, wild-type mice fed the NCD; WTHFD, wild-type mice fed the HFD; CKONCD, CyP-D–null mice fed the NCD; CKOHFD, CyP-D–null mice fed the HFD. Area under the curve (AUC) for each condition is shown in the insert. Data were analyzed as described in STATISTICAL ANALYSIS. Identical letters indicate values that are not statistically different from each other (*P* > 0.05). *C*: Adipose tissue extracts were prepared from wild-type and CyP-D–null mice fed an NCD or HFD as described and immunoblotted for ATGL, PDE3B, perilipin, the aP2 fatty acid binding protein, and the p115 Golgi protein as a loading control. *D*: Average body weight of 6 wild-type and CyP-D–null mice fed an HFD for 0, 4, and 8 weeks.

Despite the protection of adipocyte cell death, HFD in-duced adipose tissue inflammation in the CyP-D–null mice similar to wild-type mice, as indicated by a similar extent of adipose tissue macrophage infiltration (Fig. 7*A*). More-over, there was a large increase in the proportion and total number of F4/80+CD11c+ proinflammatory (M1) macro-phages with a concomitant smaller increase in F4/80+CD11c− anti-inflammatory (M2) macrophages (Fig. 7*B* and *C*). Importantly, the relative changes in these macro-phage populations were essentially identical between wild-type and CyP-D–null mice. Furthermore, the increase in adipose tissue proinflammatory M1 macrophages in the wild-type and CyP-D–null mice was consistent with the increase in the expression of proinflammatory cytokines and chemokines (Supplementary Fig. 4). These data dem-onstrate that adipose tissue inflammation and insulin re-sistance can both occur in the absence of adipocyte cell death and that CyP-D plays a necessary functional role in the HFD-induced adipocyte death pathway.

DISCUSSION

Electron microscopy analysis has demonstrated that HFD-induced adipocyte cell death has the morphologic charac-teristics of necrotic cell death (13). This includes nuclear expansion, plasma membrane fragmentation, and break-down of the large uniocular lipid droplet into smaller droplets that are present within the plasma membrane bilayer. However, other studies using TUNEL staining and caspase activation have suggested that adipocytes undergo apoptotic cell death (16,32). The basis for this difference is not clear, but our data demonstrate that a typical phar-macologic apoptotic cell-death stimulus, STS, induced apoptosis in 3T3-L1 fibroblasts but had little effect on dif-ferentiated 3T3-L1 adipocytes in caspase 3 cleavage. In contrast, two known cellular necrotic induces, ION and H_2O_2, are poor inducers of caspase 3 cleavage in 3T3-L1 adipocytes but are effective inducers of HMGB1 release, a marker that is generally believed to be a marker of ne-crotic cell death. Consistent with differentiated 3T3-L1 adipocytes being prone to undergo necrotic cell death, there is a marked induction of the essential mitochondrial protein, CyP-D, required for necrotic cell death but not apoptosis (24,33).

These data provide evidence that differentiated cultured adipocytes are biased toward necrotic cell death, but more importantly, these data suggest that CyP-D deficiency would be an effective method to prevent adipocyte cell death, independent of which specific cell-death pathway is actually involved. Therefore, to determine whether CyP-D is necessary for adipocyte cell death in vivo, we examined adipocyte cell death induced by HFD in CyP-D–null mice. Consistent with a necessary role for CyP-D in cultured adipocytes, adipocytes of CyP-D–null mice in vivo were markedly protected against HFD-induced cell death. The observation that adipocytes from CyP-D–null mice are protected against HFD-induced cell death along with the decrease in nuclear HMGB1 in HFD-treated wild-type mice provides biochemical evidence consistent with the mor-phometric analyses of adipocyte cell death in vivo.

Our data also demonstrate that inhibition of adipocyte cell death does not have any effect on HFD-induced adi-pose tissue inflammation. This was confirmed by FACS analysis and the expression of proinflammatory cytokines that was indistinguishable between adipose tissue from wild-type and CyP-D–null mice fed an HFD. In addition, we
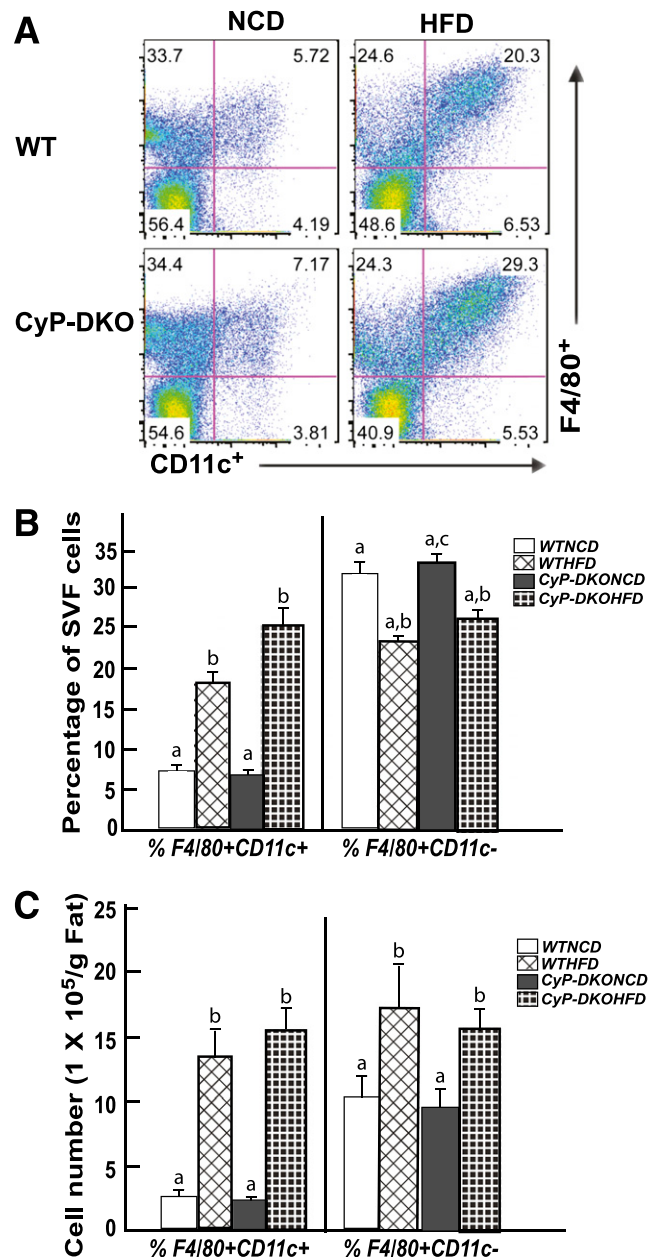
FIG. 7. CyP-D–null (KO) mice display a normal extent of HFD-induced macrophage infiltration into adipose tissue. Wild-type and CyP-D–null 9-week-old male mice were fed the NCD or HFD for 12 weeks. The stromal vascular fraction (SVF) from an entire epididymal adipose tissue fat pad was isolated and subjected to flow cytometry analysis after labeling with F4/80 and CD11c antibodies as described in RESEARCH DESIGN AND METHODS. FACS analysis of SVF isolated from epididymal ad-ipose tissue. *B*: Percentage of F4/80+CD11c+ and F4/80+CD11c− mac-rophages in epididymal adipose tissue. *C*: Total number of F4/80+CD11c+ and F480+CD11c− cells. Data shown are the mean ± standard error of the mean six mice per group and were analyzed as described in STATISTICAL ANALYSIS. Identical letters indicate values that are not statistically different from each other (*P* > 0.05).

have observed that CyP-D–null naïve macrophages are fully capable of undergoing activation to a proinflammatory state (Y.T., unpublished results). The HFD-induced inflam-matory state in both wild-type and CyP-D–null mice was also fully consistent with the development of insulin re-sistance under both conditions. Taken together, these data are consistent with the inflammatory process occurring before and independent of adipocyte cell death.

Adipose tissue inflammation occurs before adipocyte cell death, which raises the possibility that macrophage infiltration/activation and/or other immune cells provides signals that then induce adipocyte cell death. Precedence for inflammation inducing cell death comes from vascular eye development and pancreatic β-cell death in mouse models of type 1 diabetes (21,34,35). To address this issue, we took advantage of the GM-CSF–null mice, which previous studies have shown are protected against HFD-induced adipose tissue inflammation and the development of insulin resistance (22). In addition, we blocked macrophage infiltration and adipose tissue inflammation by pharmacologic treatment with liposome-clodronate (36). We confirmed these findings, and importantly, in the absence of insulin resistance and adipose tissue inflammation, the HFD GM-CSF–null mice and liposome-clodronate macrophage–ablated mice display an essentially identical extent of adipocyte cell death. These findings indicate that neither proinflammatory cytokines nor macrophages themselves play a significant role in mediating adipocyte cell death. Thus, adipocyte cell death likely results from the nutritional environment in the HFD that provides signals (direct or indirect) that are responsible for triggering the intrinsic adipocyte cell death program.

These findings also prompt the following questions:

- What is the physiologic or pathophysiologic role of HFD-induced adipocyte cell death?
- How does this relate to the role of inflammation in adipose tissue remodeling?

One possibility is that the function of macrophage infiltration is to remove by phagocytosis the triglyceride remnants that have accumulated as the result of adipocyte cell death. Because adipocyte cell death appears to be an intrinsic reactive property of adipocytes independent of macrophage inflammation, the increased levels of proinflammatory cytokines likely serve to limit triglyceride accumulation into adipocytes by inducing adipocyte insulin resistance and thereby reducing the ability of insulin to increase triglyceride storage into the surviving adipocytes that would, in turn, increase the extent of adipocyte cell death. However, other studies have reported that the rate of catecholamine-stimulated adipocyte lipolysis in obese mice and humans is decreased and has been correlated with decreased levels of hormone-sensitive lipase and ATGL (37,38).

Our data also suggest that the loss of these adipocyte lipases likely occurs as the result of adipocyte cell death and the insensitivity to catecholamines from the inability to mobilize these triglyceride remnants. On the basis of these speculations, further studies will be necessary to determine whether the adipose tissue macrophages are developing into foam cell phenotypes and whether prolonged HFD treatment increases the extent of adipose tissue triglyceride remnants with impaired mobilize of this lipid pool.

REFERENCES

1. Xu H, Barnes GT, Yang Q, et al. Chronic inflammation in fat plays a crucial role in the development of obesity-related insulin resistance. J Clin Invest 2003;112:1821–1830
2. Elgazar-Carmon V, Rudich A, Hadad N, Levy R. Neutrophils transiently infiltrate intra-abdominal fat early in the course of high-fat feeding. J Lipid Res 2008;49:1894–1903
3. Liu J, Divoux A, Sun J, et al. Genetic deficiency and pharmacological stabilization of mast cells reduce diet-induced obesity and diabetes in mice. Nat Med 2009;15:940–945
4. Winer S, Chan Y, Paltser G, et al. Normalization of obesity-associated insulin resistance through immunotherapy. Nat Med 2009;15:921–929
5. Nishimura S, Manabe I, Nagasaki M, et al. CD8+ effector T cells contribute to macrophage recruitment and adipose tissue inflammation in obesity. Nat Med 2009;15:914–920
6. Feuerer M, Herrero L, Cipolletta D, et al. Lean, but not obese, fat is enriched for a unique population of regulatory T cells that affect metabolic parameters. Nat Med 2009;15:930–939
7. Wu D, Molofsky AB, Liang HE, et al. Eosinophils sustain adipose alternatively activated macrophages associated with glucose homeostasis. Science 2011;332:243–247
8. Musi N, Goodyear LJ. Insulin resistance and improvements in signal transduction. Endocrine 2006;29:73–80
9. Solinas G, Vilcu C, Neels JG, et al. JNK1 in hematopoietically derived cells contributes to diet-induced inflammation and insulin resistance without affecting obesity. Cell Metab 2007;6:386–397
10. Zeyda M, Stulnig TM. Adipose tissue macrophages. Immunol Lett 2007;112:61–67
11. Greenberg AS, Obin MS. Obesity and the role of adipose tissue in inflammation and metabolism. Am J Clin Nutr 2006;83:461S–465S
12. Bouloumié A, Curat CA, Sengenès C, Lolmède K, Miranville A, Busse R. Role of macrophage tissue infiltration in metabolic diseases. Curr Opin Clin Nutr Metab Care 2005;8:347–354
13. Cinti S, Mitchell G, Barbatelli G, et al. Adipocyte death defines macrophage localization and function in adipose tissue of obese mice and humans. J Lipid Res 2005;46:2347–2355
14. Strissel KJ, Stancheva Z, Miyoshi H, et al. Adipocyte death, adipose tissue remodeling, and obesity complications. Diabetes 2007;56:2910–2918
15. Yang JY, Della-Fera MA, Rayalam S, Ambati S, Baile CA. Enhanced proapoptotic and anti-adipogenic effects of genistein plus guggulsterone in 3T3-L1 adipocytes. Biofactors 2007;30:159–169
16. Alkhouri N, Gornicka A, Berk MP, et al. Adipocyte apoptosis, a link between obesity, insulin resistance, and hepatic steatosis. J Biol Chem 2010;285:3428–3438
17. Frade JM, Barde YA. Microglia-derived nerve growth factor causes cell death in the developing retina. Neuron 1998;20:35–41
18. Duffield JS, Forbes SJ, Constandinou CM, et al. Selective depletion of macrophages reveals distinct, opposing roles during liver injury and repair. J Clin Invest 2005;115:56–65
19. Lang RA, Bishop JM. Macrophages are required for cell death and tissue remodeling in the developing mouse eye. Cell 1993;74:453–462
20. Diez-Roux G, Lang RA. Macrophages induce apoptosis in normal cells in vivo. Development 1997;124:3633–3638
21. Lobov IB, Rao S, Carroll TJ, et al. WNT7b mediates macrophage-induced programmed cell death in patterning of the vasculature. Nature 2005;437:417–421
22. Kim DH, Sandoval D, Reed JA, et al. The role of GM-CSF in adipose tissue inflammation. Am J Physiol Endocrinol Metab 2008;295:E1038–E1046
23. Baines CP, Kaiser RA, Purcell NH, et al. Loss of cyclophilin D reveals a critical role for mitochondrial permeability transition in cell death. Nature 2005;434:658–662

24. Devalaraja-Narashimha K, Diener AM, Padanilam BJ. Loss of cyclophilin D reveals a critical role for mitochondrial permeability transition in cell death Am J Physiol Renal Physiol 2009;297:F749–F759

25. Dranoff G, Crawford AD, Sadelain M, et al. Involvement of granulocyte-macrophage colony-stimulating factor in pulmonary homeostasis. Science 1994;264:713–716

26. Min J, Okada S, Kanzaki M, et al. Synip: a novel insulin-regulated syntaxin 4-binding protein mediating GLUT4 translocation in adipocytes. Mol Cell 1999;3:751–760

27. Li P, Lu M, Nguyen MT, et al. Functional heterogeneity of CD11c-positive adipose tissue macrophages in diet-induced obese mice. J Biol Chem 2010; 285:15333–15345

28. Pisetsky DS, Erlandsson-Harris H, Andersson U. High-mobility group box protein 1 (HMGB1): an alarmin mediating the pathogenesis of rheumatic disease. Arthritis Res Ther 2008;10:209

29. Nakayama H, Chen X, Baines CP, et al. Ca^{2+}- and mitochondrial-dependent cardiomyocyte necrosis as a primary mediator of heart failure. J Clin Invest 2007;117:2431–2444

30. Lim SY, Davidson SM, Mocanu MM, Yellon DM, Smith CC. The cardioprotective effect of necrostatin requires the cyclophilin-D component of the mitochondrial permeability transition pore. Cardiovasc Drugs Ther 2007;21:467–469

31. Schinzel AC, Takeuchi O, Huang ZH, et al. Cyclophilin D is a component of mitochondrial permeability transition and mediates neuronal cell death after focal cerebral ischemia. Proc Natl Acad Sci U S A 2005;102:12005–12010

32. Fischer-Posovszky P, Hebestreit H, Hofmann AK, et al. Role of CD95-mediated adipocyte loss in autoimmune lipodystrophy. J Clin Endocrinol Metab 2006;91:1129–1135

33. Nakagawa T, Shimizu S, Watanabe T, et al. Cyclophilin D-dependent mitochondrial permeability transition regulates some necrotic but not apoptotic cell death. Nature 2005;434:652–658

34. Cnop M, Welsh N, Jonas JC, Jörns A, Lenzen S, Eizirik DL. Mechanisms of pancreatic beta-cell death in type 1 and type 2 diabetes: many differences, few similarities. Diabetes 2005;54(Suppl. 2):S97–S107

35. Eizirik DL, Mandrup-Poulsen T. A choice of death—the signal-transduction of immune-mediated beta-cell apoptosis. Diabetologia 2001;44:2115–2133

36. Kosteli A, Sugaru E, Haemmerle G, et al. Weight loss and lipolysis promote a dynamic immune response in murine adipose tissue. J Clin Invest 2010; 120:3466–3479

37. Langin D, Dicker A, Tavernier G, et al. Adipocyte lipases and defect of lipolysis in human obesity. Diabetes 2005;54:3190–3197

38. Steinberg GR, Kemp BE, Watt MJ. Adipocyte triglyceride lipase expression in human obesity. Am J Physiol Endocrinol Metab 2007;293:E958–E964